

Detect edge degeneracy in interacting topological insulators using entanglement entropy

Da Wang,¹ Shenglong Xu,¹ Yu Wang,² and Congjun Wu¹

¹*Department of Physics, University of California, San Diego, California 92093, USA*

²*School of Physics and Technology, Wuhan University, Wuhan 430072, China*

Edge degeneracy is closely related to the bulk topological property of a topological insulator. We propose to detect the edge degeneracy with the help of entanglement entropy. Combining periodic and open boundary conditions, we define an edge state entanglement entropy $S_{n,\text{edge}}$, which is used to identify the edge degeneracy. Using fermionic quantum Monte Carlo algorithm, we investigate two models: 1D Su-Schrieffer-Heeger-Hubbard model and 2D Kane-Mele-Hubbard model. In topologically nontrivial phases of these two models, we find $S_{2,\text{edge}}$ is quantized to $\log 2$, which is half of the non-interacting result and indicates the interaction effect. In 2D, such a nonzero $S_{2,\text{edge}}$ also contributes a subleading term in the area law of entanglement entropy for a cylinder geometry.

PACS numbers: 03.65.Vf, 03.65.Ud, 02.70.Ss, 71.10.Fd

Introduction— Topologically nontrivial ground states of gapped systems are an interesting topic in condensed matter physics. They are classified into two kinds with either long or short range entanglement. The long range entangled topological state can be characterized by its ground state degeneracy on a closed manifold [1]. Similarly, the short range entangled topological insulator/superconductor [2] can be characterized by its edge degeneracy on a physical boundary. (For clarity, in this paper, we use *topological insulator* to represent the general short range entangled topological states, but not only the time reversal invariant (TRI) \mathbb{Z}_2 quantum spin Hall insulator [3].) For non-interacting topological insulators, such an edge degeneracy comes directly from zero energy edge mode, which is protected by its bulk topological property through the bulk-edge correspondence [4, 5][6]. However, when interaction exists, the single particle picture does not hold any more. The usual bulk-edge correspondence should be understood as the relation between bulk topological property and the many body ground state degeneracy on the edge. In fact, this idea has been borrowed from some topological classification works on interacting topological insulators [7, 8]. In recent years, interaction effect on topological insulators has been broadly studied [9–13]. Especially, the non-interacting topological band insulating phase is found to persist with nonzero interaction until it reaches another phase for large enough interaction [12, 13]. More systematically, interacting fermions have been classified with respect to different symmetries [7, 8, 14]. For the class of TRI topological insulator, the topological number is found to have a relationship with the single particle Green's function [15] and have been obtained from different approaches [16, 17]. In this work, we provide another point of view to detect the edge degeneracy using entanglement entropy (EE).

Quantum entanglement, as a concept in quantum information, provides a peculiar perspective to investigate quantum many body physics [18]. It measures nonlo-

cal correlation between two parts A and B of a bipartite system through the reduced density matrix $\rho_A = \text{Tr}_B(\rho_{A \cup B})$, which can be used to define von Neumann EE $S_v = -\text{Tr}(\rho_A \log \rho_A)$. Usually with only short range entanglement, EE respects an area law: proportional to the area/length of the boundary between A and B (entanglement cut). However, this relation can break down. In a quantum critical region, the EE shows logarithmic dependence on the subsystem size due to divergence of coherence length [19]; In a long range entangled topological order, a negative subleading term named topological entanglement entropy (TEE) [20] is related to its degenerate ground states. TEE has been successfully used to identify different topological orders such as quantum spin liquids [21, 22]. On the other hand, for short range entangled topological insulators, TEE is found to be zero in torus. In non-interacting case, single particle entanglement spectrum [23] exhibits 'zero mode' and has been used to identify topological insulators [24, 25]. However, when interaction is turned on, the single particle picture also loses its meaning. In this paper, we propose a quantity $S_{n,\text{edge}}$ (defined in Eq. 2) to measure the edge degeneracy for both non-interacting and interacting topological insulators.

This work is motivated by a recently developed algorithm using fermionic determinant Quantum Monte Carlo (QMC) to calculate Renyi EE $S_n = -\ln \text{Tr}(\rho_A^n)/(n-1)$ [26]. In this paper, we employ this algorithm to investigate edge degeneracy of fermionic interacting topological insulators by measuring $S_{2,\text{edge}}$ in both one and two dimensional systems. We first explain our methodology using the Su-Schrieffer-Heeger-Hubbard (SSH) model [27]. We find that $S_{2,\text{edge}}$ characterizes different topological phases. In the topologically nontrivial phase, Hubbard U is found to reduce $S_{2,\text{edge}}$ from $2 \log 2$ to $\log 2$, corresponding to edge degeneracy from 4 to 2 in thermodynamic limit. In 2D, such a nonzero $S_{2,\text{edge}}$ also contributes a subleading term in the EE area law, as we observe in the Kane-Mele-Hubbard

(KMH) model [28] for a cylinder geometry. Moreover, $S_{2,\text{edge}}$ shows even-odd dependence on the entanglement cut size, in agreement with the helical liquid behavior on the edge.

SSH model— First we consider the 1D SSHH model,

$$H_{SSH} = - \sum_{i=1, \sigma}^{2L} [t + \delta t(-1)^i] c_{i\sigma}^\dagger c_{i+1, \sigma} + H.c. + \sum_{i=1}^{2L} \frac{U}{2} (n_i - 1)^2, \quad (1)$$

where $\sigma = \uparrow, \downarrow$, $n_i = \sum_{\sigma} c_{i\sigma}^\dagger c_{i\sigma}$, δt controls the hopping dimerization strength and the average hopping t is set 1 below. The second line gives the Hubbard repulsion U between opposite spins on the same site.

When $U = 0$, this model is well known to have two topologically distinct ground states, characterized by Berry phase 0 ($\delta t > 0$) and π ($\delta t < 0$) respectively. (Site i (odd) and $i + 1$ are combined as a unit cell.) In the topologically nontrivial phase with $\delta t < 0$, Berry phase π guarantees the existence of a zero energy mode on one end for each spin [24], see the inset of Fig. 1(a). Next, we divide the whole chain into two parts, one with $[1, L]$ as the subsystem A and the other half $[L + 1, 2L]$ as the environment B. Using the truncated correlation matrix $\mathcal{C}_{ij\sigma} = \langle c_{i\sigma}^\dagger c_{j\sigma} \rangle$ with $i, j \in A$, the Renyi EE can be obtained [29] as $S_n = -\frac{1}{n-1} \sum \log(f_{i\sigma}^n)$, where $f_{i\sigma}$ are eigenvalues of $\mathcal{C}_{ij\sigma}$. We plot S_2 with both periodic boundary condition (PBC) and open boundary condition (OBC) in Fig. 1(a). Neither PBC nor OBC gives quantized EE in the whole regime because of short range entanglement near the entanglement cut [24]. However, we find that by subtracting these two results (half of $S_{n,\text{PBC}}$ is subtracted because of two entanglement cuts in PBC but only one entanglement cut in OBC), we gain a quantity:

$$S_{n,\text{edge}} = S_{n,\text{OBC}} - \frac{S_{n,\text{PBC}}}{2}, \quad (2)$$

which shows almost quantized behavior. Here n can be chosen as any value. ($n = 1$ means von Neumann EE.) In this work, we only consider $n = 2$, since S_2 is most easy to obtain by QMC. Eq. 2 is a central quantity in this paper. It measures the nonlocal entanglement between the edge states on two physical boundaries. In the $U = 0$ case, two spins are decoupled. When $\delta t < 0$ for each spin σ , two zero modes $\gamma_{(L,R)\sigma}$ at two ends are coupled together through an effective hopping $t_{\text{eff}} \sim \exp(-\delta t L)$. Then their bonding state $(\gamma_{L\sigma}^\dagger - \gamma_{R\sigma}^\dagger)|0\rangle$ contributes a $\log 2$ to $S_{n,\text{edge}}$. Therefore, $S_{2,\text{edge}} = 2 \log 2$ when $\delta t < 0$ while $S_{2,\text{edge}} = 0$ when $\delta t > 0$, as shown in Fig. 1(a). This fact motivates us to use it as a topological index. It should be noted that t_{eff} goes to zero for infinite L , in which case the zero modes on one edge become isolated from the ones on the other edge. Such zero modes give rise to many body ground state 4-fold degeneracy, also leading to $2 \log 2$ in thermodynamic entropy at zero

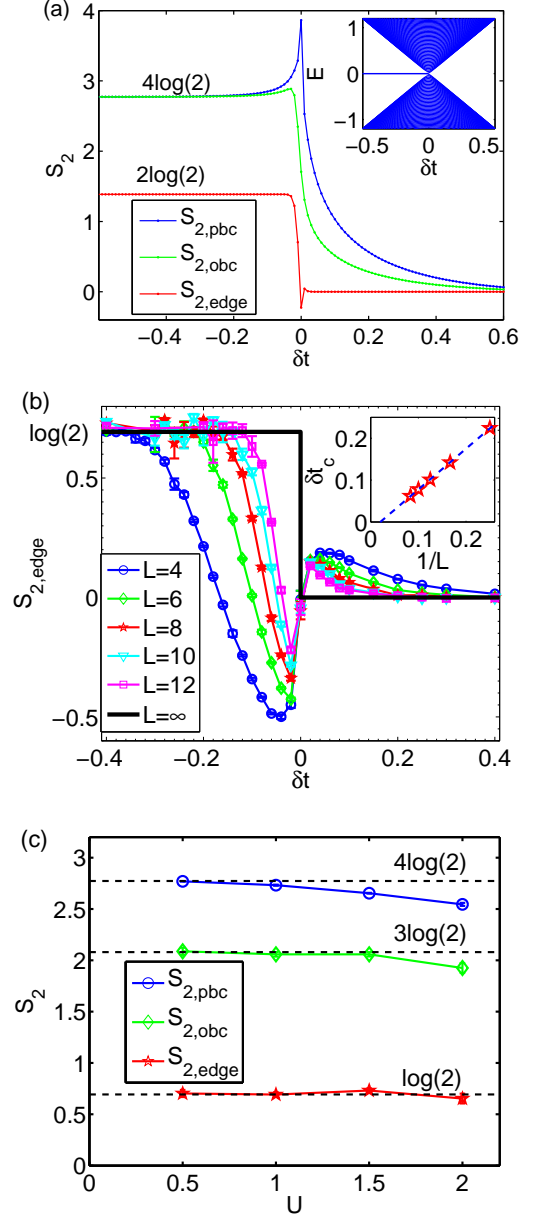


FIG. 1. 2nd order Renyi EE of the SSHH model. (a) Results of $U = 0$ on a $L = 40$ chain. The inset shows the energy spectrum with OBC. (b) $S_{2,\text{edge}}$ obtained by QMC as a function δt when $U = 1$. Different lattice sizes from $L = 4$ to $L = 12$ are used. The inset plots the extrapolation of δt_c defined as $S_{2,\text{edge}}(t_c) = \log 2/2$ vs $1/L$. (c) S_2 vs U at fixed $\delta t = -0.2$. In QMC calculations, the projection time $\beta = 4L$, and the time step $\Delta\tau = 0.05$.

temperature [30]. This explains the relation between entanglement entropy and the ground state degeneracy \mathcal{D} on one physical boundary:

$$\log(\mathcal{D}) = \lim_{L \rightarrow \infty} S_{n,\text{edge}}(L). \quad (3)$$

This relation tells us $S_{n,\text{edge}}(L)$ converges to the same value independent of n . Therefore, it is sufficient for us

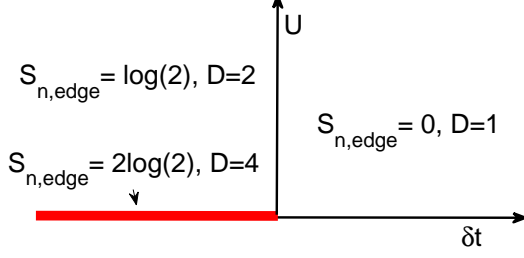


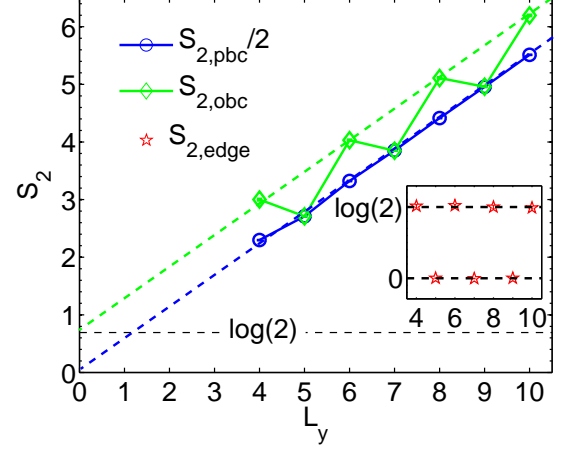
FIG. 2. Phase diagram of SSH model.

to calculate S_2 to detect edge degeneracy.

When Hubbard U is turned on, we use zero temperature projector QMC [31] combined with the new developed algorithm to calculate S_2 [26] in two different boundary conditions. Due to particle-hole symmetry, the half-filled SSH model is free of sign problem. In Fig. 1(b), we plot $S_{2,\text{edge}}$ vs δt with different sizes when $U = 1$. For each L , $S_{2,\text{edge}}$ saturates to $\log 2$ and 0 respectively in two limits with large $|\delta t|$. When system size L increases, the transition becomes more and more sharp. In the inset, we plot transition point δt_c defined at $S_{2,\text{edge}}(\delta t_c) = \log 2/2$ as a function of $1/L$. δt_c extrapolates to zero in the limit of $L \rightarrow \infty$. Thus we deduce the result of $L = \infty$. This result is the same as $U = 0$ in Fig. 1(a), except $S_{2,\text{edge}} = \log 2$ but not $2\log 2$. This means that the edge degeneracy is reduced from 4 to 2 by Hubbard U , i.e. double occupation and empty states are projected out. For finite L , the effective coupling t_{eff} between two edges will break the double degeneracy and produce a singlet ground state $[\gamma_{L\uparrow}^\dagger \gamma_{R\downarrow}^\dagger - \gamma_{L\downarrow}^\dagger \gamma_{R\uparrow}^\dagger] |0\rangle$, as long as $U \gg t_{\text{eff}}$. This singlet state leads to $S_{2,\text{edge}} = \log 2$. Due to the exponential decay of t_{eff} , $S_{2,\text{edge}}$ suffers very little finite size effect and converges to $\log(\mathcal{D})$ quickly without the need of large lattice size, which is very convenient for numerical calculations.

We have also checked different values of U ranging from 0.5 to 2. The results are shown in Fig. 1(c). Although $S_{2,\text{pbc}}$ and $S_{2,\text{obc}}$ are not quantized, which is clearer for larger U , $S_{2,\text{edge}}$ is pinned at $\log 2$ with regardless of U , in agreement with the above analysis. In Fig. 2, we build up the phase diagram of the SSH model using $S_{n,\text{edge}}$ and edge degeneracy. Similar phase diagram has been obtained by calculating the bulk topological number $\mathcal{Z} = 0(2)$ for $\delta t > 0(< 0)$ using Green's functions extracted from density matrix renormalization group [16]. Our study here further indicates the edge behavior: in the topologically nontrivial region, the edge degeneracy is reduced from 4 to 2 by Hubbard interaction [8].

In the case of large U , the SSH model is equivalent to the spin 1/2 Heisenberg-Peierls model $H = \sum_i J_i \mathbf{S}_i \cdot \mathbf{S}_{i+1}$, where $J_i = J(J')$ for odd(even) bond respectively. Our study shows $J' < J$ and $J' > J$ belong to topologically distinct phases. When $J < J'$, there is

FIG. 3. 2nd order Renyi entanglement entropy of KMH model vs L_y . In the inset, $S_{2,\text{edge}}$ is plotted. The parameters are $L_x = 6$, $U = 1$, $\lambda = 0.2$, $\beta = 10L_y$, $\Delta\tau = 0.05$.

a free local moment at one end resulting in double edge degeneracy. The transition occurs at $J = J'$, in consistent with the critical behavior of the spin 1/2 Heisenberg model [32, 33].

KMH model— Next, we move to 2D and investigate the KMH model on a honeycomb lattice,

$$H_{\text{KMH}} = - \sum_{\langle i,j \rangle, \sigma} t c_{i\sigma}^\dagger c_{j\sigma} + \sum_{\langle\langle i,j \rangle\rangle, \sigma} i\lambda c_{i\sigma}^\dagger \sigma c_{j\sigma} + \sum_i \frac{U}{2} (n_i - 1)^2, \quad (4)$$

where λ is the second nearest neighbor spin-orbit coupling, $\sigma = 1(\uparrow), -1(\downarrow)$, and t is chosen as 1 below. This model is also free of sign problem, and thus enables us to perform high precision numerical studies [13]. In the following, we choose PBC along the zigzag direction, defined as y -direction. While along x -direction (armchair direction), both PBC and OBC are considered and form two different geometries: torus and cylinder. In the following, we bipartite the lattice into subsystem A with $1 \leq x \leq L/2$ and environment B with $L/2 + 1 \leq x \leq L$ to study their entanglement.

Our QMC results of the KMH model are given in Fig. 3. $S_{2,\text{pbc}}$ exhibits a standard area law, i.e. $S_{2,\text{pbc}} \propto L_y$. But $S_{2,\text{obc}}$ shows an even-odd oscillating behavior. As a result, using Eq. 2 we obtain $S_{2,\text{edge}} = \log 2(0)$ for even(odd) L_y , respectively, as shown in the inset. On the other hand, we can also obtain $S_{2,\text{edge}}$ by doing extrapolation using the OBC results with even L_y . $S_{2,\text{edge}}$ appears as the subleading term of the area law $S_{2,\text{obc}} \approx \alpha L_y + S_{2,\text{edge}}$. This area law is robust even though the lattice size is not so large. Such a subleading term is reminiscent of the TEE in long range entangled quantum topological orders [20], e.g. quantum spin liquid states [21, 22]. In analogy to TEE, we propose to use $S_{n,\text{edge}}$ to characterize the short range entangled topo-

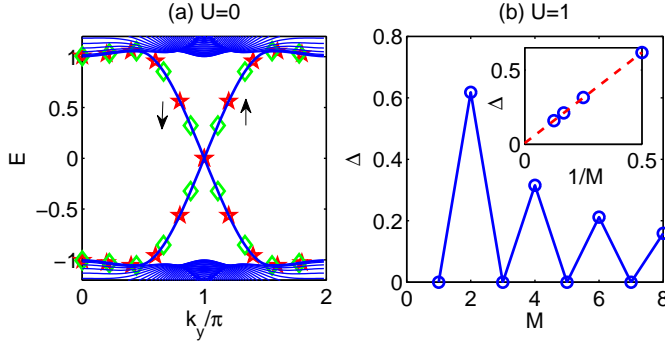


FIG. 4. Helical liquid behavior at the edge of KMH model. (a) Single particle energy spectrum at $U = 0$. Red and blue symbols mark the edge states with $L = 10$ and $L = 9$ respectively. (b) The many body energy gap Δ vs size M for the effective model Eq. 5 with $U = 2\pi v_F = 1$. The inset plots Δ vs $1/M$ for only even M .

logical insulators. Both TEE and $S_{n,\text{edge}}$ are related to the ground state degeneracy, but account for bulk and edge states respectively.

Next, we explain the origin of the nonzero $S_{2,\text{edge}}$ by analyzing the edge degeneracy. When $U = 0$, such a behavior is a direct consequence of the zero energy edge states. Similar phenomena has also been observed in Kitaev model [34], and non-interacting triplet topological superconductors [35]. In Fig. 4(a), we plot the energy spectrum with open boundary as a function of k_y which is a good quantum number due to PBC along y direction. The zero mode at $k_y = \pi$ can (cannot) be chosen for even(odd) L_y . Thus the many body ground state degeneracy changes between 4 and 1 alternatively by changing L_y . However, when $U \neq 0$, such a single particle picture does not hold any more. Interaction effect has to be taken into account exactly to investigate the many body edge degeneracy. We study this problem in an effective edge Hamiltonian: a helical liquid [36],

$$H_{hl} = \sum_{k,\sigma} v_F \sigma k c_{k\sigma}^\dagger c_{k\sigma} + \frac{U}{M} \sum_{kk'q} c_{k+q\uparrow}^\dagger c_{k\uparrow} c_{k'-q\downarrow}^\dagger c_{k'\downarrow} \quad (5)$$

where we define $k = \frac{\pi}{M}(2i - M - 1)$ ($i = 0, \dots, M - 1$). Here Hubbard U term has been written in momentum space. Notice that odd M here corresponds to even L_y . We use exact diagonalization method to numerically solve the energy levels with $M \leq 8$ and plot the

energy gaps in Fig. 4(b). For odd M , $\Delta = 0$ corresponds to a double degeneracy, in agreement with the QMC result $S_{2,\text{edge}} = \log 2$ for even L_y ; For even M , the ground state has no degeneracy, thus $S_{2,\text{edge}} = 0$. But the gap decreases to zero as M increases as shown in the inset. This gapless behavior in thermodynamic limit has been obtained from Bosonization analysis [36], which shows that forward scattering does not open a gap in a helical liquid. Therefore, the even-odd oscillating behavior will not cause ambiguity in thermodynamic limit.

Recently, the bulk \mathbb{Z}_2 topological number of the KMH model has been obtained using single particle Green's functions in QMC calculations [17]. It is found that non-interacting \mathbb{Z}_2 number is not changed by interaction U , indicating the topological insulating state persists into finite U until Mott transition occurs accompanied by antiferromagnetic long range order at large U [13]. Our study confirms the interacting topological state by identifying the edge degeneracy which is reduced from 4 to 2 by U even though their bulk \mathbb{Z}_2 numbers are the same.

Before closing this paper, some remarks are in order. (1) Our QMC calculations are only performed at small and medium U . When U goes up, the QMC numerical error of EE increases significantly [26]. One needs to pay lots of effort to obtain reliable EE for large U . Very recently, a new QMC algorithm using replica technique was proposed for fermionic systems [37], which may be more stable in large U regime and can help us study the Mott transition regime in the future. (2) If the third nearest neighbor hopping is added to the KMH model, two Dirac nodes can be produced at $k_y = 0$ and π respectively on an edge [17]. In this case, any small U will gap out the edge states due to Umklapp scattering [36] of the Hubbard interaction. Therefore, we expect $S_{2,\text{edge}} = 0$, in consistent with the meaning of \mathbb{Z}_2 topological insulator.

Summary— In this paper, we propose a quantized quantity $S_{n,\text{edge}}$ to detect the edge degeneracy in topological insulators. Using the fermionic quantum Monte Carlo algorithm, we investigate 1D SSH model and 2D KMH model. In both topologically nontrivial phases, we find $S_{2,\text{edge}}$ is quantized to $\log 2$, which is half of the non-interacting result and indicates the interaction effect. In 2D, such a nonzero $S_{n,\text{edge}}$ also contributes a subleading term in the EE area law for a cylinder geometry.

Acknowledgments— D. W. thanks Zhoushen Huang and Xiao Chen for many helpful discussions. This work is supported by NSF DMR-1105945 and AFOSR FA9550-11-1-0067(YIP).

[1] X. G. Wen and Q. Niu, *Phys. Rev. B* **41**, 9377 (1990).
[2] A. P. Schnyder, S. Ryu, A. Furusaki, and A. W. Ludwig, *Phys. Rev. B* **78**, 195125 (2008).
[3] M. Z. Hasan and C. L. Kane, *Rev. Mod. Phys.* **82**, 3045 (2010); X.-L. Qi and S.-C. Zhang, *Rev. Mod. Phys.* **83**, 1057 (2011).

[4] Y. Hatsugai, *Phys. Rev. Lett.* **71**, 3697 (1993); S. Ryu and Y. Hatsugai, *Phys. Rev. Lett.* **89**, 077002 (2002).
[5] X.-L. Qi, Y.-S. Wu, and S.-C. Zhang, *Phys. Rev. B* **74**, 045125 (2006).
[6] In some special cases, there is no zero mode on an open boundary even in a topologically nontrivial state, e.g. Refs. [38, 39]. Then the bulk-edge correspondence should

- be generalized by introducing twisted boundary condition [5].
- [7] L. Fidkowski and A. Kitaev, *Phys. Rev. B* **83**, 075103 (2011); X.-L. Qi, *New J. Phys.* **15**, 065002 (2013); H. Yao and S. Ryu, *Phys. Rev. B* **88**, 064507 (2013).
 - [8] E. Tang and X.-G. Wen, *Phys. Rev. Lett.* **109**, 096403 (2012).
 - [9] S. Raghu, X.-L. Qi, C. Honerkamp, and S.-C. Zhang, *Phys. Rev. Lett.* **100**, 156401 (2008).
 - [10] M. Dzero, K. Sun, V. Galitski, and P. Coleman, *Phys. Rev. Lett.* **104**, 106408 (2010); D. J. Kim, S. Thomas, T. Grant, J. Botimer, Z. Fisk, and J. Xia, *Sci. Rep.* **3**, (2013); X. Zhang, N. P. Butch, P. Syers, S. Ziemak, R. L. Greene, and J. Paglione, *Phys. Rev. X* **3**, 011011 (2013).
 - [11] A. Shitade, H. Katsura, J. Kuneš, X.-L. Qi, S.-C. Zhang, and N. Nagaosa, *Phys. Rev. Lett.* **102**, 256403 (2009); X. Zhang, H. Zhang, J. Wang, C. Felser, and S.-C. Zhang, *Science* **335**, 1464 (2012).
 - [12] S. Rachel and K. Le Hur, *Phys. Rev. B* **82**, 075106 (2010); C. N. Varney, K. Sun, M. Rigol, and V. Galitski, *Phys. Rev. B* **82**, 115125 (2010).
 - [13] M. Hohenadler, T. C. Lang, and F. F. Assaad, *Phys. Rev. Lett.* **106**, 100403 (2011); D. Zheng, G.-M. Zhang, and C. Wu, *Phys. Rev. B* **84**, 205121 (2011); S.-L. Yu, X. C. Xie, and J.-X. Li, *Phys. Rev. Lett.* **107**, 010401 (2011); J. Yuan, J.-H. Gao, W.-Q. Chen, F. Ye, Y. Zhou, and F.-C. Zhang, *Phys. Rev. B* **86**, 104505 (2012).
 - [14] X. Chen, Z.-X. Liu, and X.-G. Wen, *Phys. Rev. B* **84**, 235141 (2011); A. M. Turner, F. Pollmann, and E. Berg, *Phys. Rev. B* **83**, 075102 (2011); Y.-M. Lu and A. Vishwanath, *Phys. Rev. B* **86**, 125119 (2012); Z.-C. Gu and X.-G. Wen, (2012), [arXiv:1201.2648](#); C. Wang, A. C. Potter, and T. Senthil, *Science* **343**, 629 (2014).
 - [15] Z. Wang, X.-L. Qi, and S.-C. Zhang, *Phys. Rev. Lett.* **105**, 256803 (2010); L. Wang, X. Dai, and X. C. Xie, *Phys. Rev. B* **84**, 205116 (2011); Z. Wang and S.-C. Zhang, *Phys. Rev. X* **2**, 031008 (2012).
 - [16] S. R. Manmana, A. M. Essin, R. M. Noack, and V. Gurarie, *Phys. Rev. B* **86**, 205119 (2012); L. Wang, H. Jiang, X. Dai, and X. C. Xie, *Phys. Rev. B* **85**, 235135 (2012); M. A. N. Araújo, E. V. Castro, and P. D. Sacramento, *Phys. Rev. B* **87**, 085109 (2013); L. Wang, A. A. Soluyanov, and M. Troyer, *Phys. Rev. Lett.* **110**, 166802 (2013).
 - [17] H.-H. Hung, L. Wang, Z.-C. Gu, and G. A. Fiete, *Phys. Rev. B* **87**, 121113 (2013); H.-H. Hung, V. Chua, L. Wang, and G. A. Fiete, (2013), [arXiv:1307.2659](#); T. C. Lang, A. M. Essin, V. Gurarie, and S. Wessel, *Phys. Rev. B* **87**, 205101 (2013).
 - [18] L. Amico, R. Fazio, A. Osterloh, and V. Vedral, *Rev. Mod. Phys.* **80**, 517 (2008); J. Eisert, M. Cramer, and M. B. Plenio, *Rev. Mod. Phys.* **82**, 277 (2010).
 - [19] G. Vidal, J. I. Latorre, E. Rico, and A. Kitaev, *Phys. Rev. Lett.* **90**, 227902 (2003).
 - [20] A. Kitaev and J. Preskill, *Phys. Rev. Lett.* **96**, 110404 (2006); M. Levin and X.-G. Wen, *Phys. Rev. Lett.* **96**, 110405 (2006).
 - [21] Y. Zhang, T. Grover, and A. Vishwanath, *Phys. Rev. Lett.* **107**, 067202 (2011); Y. Zhang, T. Grover, A. Turner, M. Oshikawa, and A. Vishwanath, *Phys. Rev. B* **85**, 235151 (2012).
 - [22] S. Yan, D. A. Huse, and S. R. White, *Science* **332**, 1173 (2011); H.-C. Jiang, Z. Wang, and L. Balents, *Nat. Phys.* **8**, 902 (2012); H.-C. Jiang, H. Yao, and L. Balents, *Phys. Rev. B* **86**, 024424 (2012).
 - [23] H. Li and F. D. M. Haldane, *Phys. Rev. Lett.* **101**, 010504 (2008).
 - [24] S. Ryu and Y. Hatsugai, *Phys. Rev. B* **73**, 245115 (2006).
 - [25] L. Fidkowski, *Phys. Rev. Lett.* **104**, 130502 (2010).
 - [26] T. Grover, *Phys. Rev. Lett.* **111**, 130402 (2013); F. F. Assaad, T. C. Lang, and F. Parisen Toldin, *Phys. Rev. B* **89**, 125121 (2014).
 - [27] W. P. Su, J. R. Schrieffer, and A. J. Heeger, *Phys. Rev. Lett.* **42**, 1698 (1979).
 - [28] C. L. Kane and E. J. Mele, *Phys. Rev. Lett.* **95**, 146802 (2005).
 - [29] I. Peschel, *J. Phys. A: Math. Gen.* **36**, L205 (2003); S.-A. Cheong and C. L. Henley, *Phys. Rev. B* **69**, 075111 (2004).
 - [30] We use zero temperature thermodynamic entropy to represent the entropy of a mixed state with decoherent superposition of different pure states.
 - [31] F. F. Assaad and H. G. Evertz, “Computational many-particle physics,” (2008).
 - [32] J. des Cloizeaux and J. J. Pearson, *Phys. Rev.* **128**, 2131 (1962).
 - [33] F. D. M. Haldane, *Phys. Rev. Lett.* **50**, 1153 (1983).
 - [34] H. Yao and X.-L. Qi, *Phys. Rev. Lett.* **105**, 080501 (2010).
 - [35] T. P. Oliveira, P. Ribeiro, and P. D. Sacramento, ArXiv e-prints (2013), [arXiv:1312.7782](#).
 - [36] C. Wu, B. A. Bernevig, and S.-C. Zhang, *Phys. Rev. Lett.* **96**, 106401 (2006).
 - [37] P. Broecker and S. Trebst, ArXiv e-prints (2014), [arXiv:1404.3027](#).
 - [38] A. M. Turner, Y. Zhang, and A. Vishwanath, *Phys. Rev. B* **82**, 241102 (2010); T. L. Hughes, E. Prodan, and B. A. Bernevig, *Phys. Rev. B* **83**, 245132 (2011).
 - [39] Z. Huang and D. P. Arovas, (2012), [arXiv:1205.6266](#).